20. Kaminski, A. *et al.* Quasiparticles in the superconducting state of $Bi_2Sr_2CaCu_2O_{8+\delta}$. *Phys. Rev. Lett.* **84,** 1788–1791 (2000).
21. Millis, A. J. & Drew, H. D. Quasiparticles in high temperature superconductors: consistency of angle resolved photoemission and optical conductivity. Preprint at ⟨http://www.arXiv.org/cond-mat/0303018⟩ (2003).
22. Schachinger, E., Tu, J. J. & Carbotte, J. P. Angle-resolved photoemission spectroscopy and optical renormalizations: phonons or spin fluctuations. *Phys. Rev. B* **67,** 214508 (2003).
23. Dai, P. *et al.* The magnetic excitations spectrum and thermodynamics of high-T_c superconductors. *Science* **284,** 1344–1347 (1999).
24. Hwang, J. *et al.* Marginal Fermi liquid analysis of 300 K reflectance of $Bi_2Sr_2CaCu_2O_{8+}\delta$. Preprint at ⟨http://www.arXiv.org/cond-mat/0306250⟩ (2003).
25. Chakravarty, S. *et al.* Hidden order in the cuprates. *Phys. Rev. B* **63,** 094503 (2001).
26. Loram, J. W. *et al.* The condensation energy and pseudogap energy scale of Bi:2212 from electronic specific heat. *Physica C* **341–348,** 831–834 (2000).
27. Shibauchi, T. *et al.* Closing the pseudogap by Zeeman splitting in $Bi_2Sr_2CaCu_2O_{8+y}$ at high magnetic fields. *Phys. Rev. Lett.* **86,** 5763–5766 (2001).
28. Takenaka, K., Mizuhashi, K., Takagi, H. & Uchida, S. Interplane charge transport in $YBa_2Cu_3O_{7-y}$: Spin gap effect on in-plane and out-of-plane resistivity. *Phys. Rev. B* **50,** 6534–6537 (1994).
29. Homes, C. C. *et al.* Technique for measuring the reflectance of irregular, submillimeter-sized samples. *Appl. Opt.* **32,** 2976–2983 (1993).
30. Eisaki, H. *et al.* Effect of chemical inhomogeneity in the bismuth-based copper oxide superconductors. *Phys. Rev. B* (in the press); preprint at ⟨http://www.arXiv.org/cond-mat/0312429⟩ (2004).

Acknowledgements This work has been supported by the Canadian Natural Science and Engineering Research Council and the Canadian Institute of Advanced Research. We thank H. Eisaki and M. Greven for supplying us with several crystals. Their work at Stanford University was supported by the Department of Energy's Office of Basic Sciences, Division of Materials Science. The work at Brookhaven was supported in part by the Department of Energy. We thank D. N. Basov, J. P. Carbotte, G. M. Luke and M. R. Norman for discussions.

Competing interests statement The authors declare that they have no competing financial interests.

Correspondence and requests for materials should be addressed to T.T. (timusk@mcmaster.ca).

Clarifying the glass-transition behaviour of water by comparison with hyperquenched inorganic glasses

Yuanzheng Yue[1] **& C. Austen Angell**[2]

[1]*Section of Chemistry, Department of Life Sciences, Aalborg University, DK-9000 Aalborg, Denmark*
[2]*Department of Chemistry and Biochemistry, Arizona State University, Tempe, Arizona 85287, USA*

The formation of glasses is normal for substances that remain liquid over a wide temperature range (the 'good glassformers') and can be induced for most liquids if cooling is fast enough to bypass crystallization. During reheating but still below the melting point, good glassformers exhibit glass transitions as they abruptly transform into supercooled liquids, whereas other substances transform directly from the glassy to the crystalline state. Whether water exhibits a glass transition before crystallization has been much debated over five decades[1,2–6]. For the last 20 years, the existence of a glass transition at 136 K (ref. 3) has been widely accepted[2–4], but the transition exhibits qualities difficult to reconcile with our current knowledge of glass transitions[2,5,6]. Here we report detailed calorimetric characterizations of hyperquenched inorganic glasses that, when heated, do not crystallize before reaching their glass transition temperatures. We compare our results to the behaviour of glassy water and find that small endothermic effects, such as the one attributed to the glass transition of water, are only a 'shadow' of the real glass transition occurring at higher temperatures, thus substantiating the conclusion[6] that the glass transition of water cannot be probed directly.

Glassy water is the most abundant form of water in the Universe, found as thin films condensed on the interstellar dust particles that constitute the major component of comets[7]. This material, amorphous solid water (ASW), like hyperquenched glassy water (HQGW), is in a configurationally excited state (or state of high fictive temperature), relative to glasses formed by standard ($20\,K\,min^{-1}$) cooling. To release the excitation enthalpy, the glass is usually annealed at temperatures where it does not crystallize. There is controversy about the state to which it is able to relax before crystallization occurs[1–11].

Until recently it was believed that ASW, HQGW and low-density amorphous water (LDA) all reach the internally equilibrated (or metastable liquid) state, so that it is a viscous liquid that is crystallizing. Observation of a weak endothermic effect at 136 K attributed to a glass transition[3], penetration of millimetres-thick samples of LDA water (a state close in character to ASW) by a blunt probe at a temperature 14 K above the LDA glass transition temperature T_g of 129 K (ref. 8), and liquid-like diffusion at 150 K (ref. 9) support this view. Water, it was concluded, is a very fragile liquid, not only near its melting point[10], but also near T_g (refs 9, 11).

The 136 K T_g is found by differential scanning calorimetry (DSC) using a heating rate of $10\,K\,min^{-1}$, but only after annealing the sample to avoid obscuring the endothermic signal by the release of the excitation enthalpy of the glass[3,13,14]. (One important exception, where an endothermic effect is observed without prior sample annealing, is discussed below[12].) One difficulty with attributing the endotherm effect to the water T_g is that it is exceptionally weak: the jump in the heat capacity C_p of only $1.6\,J\,mol^{-1}\,K^{-1}$ (ref. 14) is some 14 times smaller than the value expected at this temperature, according to extrapolations of data from unambiguous glass transitions in binary aqueous solutions that are good glassformers[2,15]. This implies either that water undergoes a fragile-to-strong liquid transition in the experimentally inaccessible part of its phase diagram[10], or that the 136 K endotherm is not caused by a glass transition at this temperature.

In this context, it is useful to consider that previous work failed to find evidence for a T_g endotherm[5,16]; successful observation of the endotherm at 136 K required initial annealing of the glass for extended periods of 95 min (ref. 3) or 90 min (ref. 14), at about 6 K below the temperature at which the endothermic effect was subsequently identified. However, if the relaxation of the glassformer in question is strongly non-exponential, then annealing a quenched glass or even a standard glass far below its T_g is known to promote the appearance of a 'sub-T_g peak' during a subsequent DSC upscan[17,18]. The shape of the observed endotherm at 136 K does in fact differ from the shape predicted for sub-T_g peaks using phenomenological models[17]; but modelling comparisons have not been made for hyperquenched glasses (HQGs) and the models are known to fail for systems far from equilibrium[19].

From a recent comparison[5] of the relaxation exotherm of unannealed HQGW with those of glassformers that do not crystallize it was concluded that the endotherm observed after annealing could not be due to a glass transition at 136 K, but could be due to relaxation of localized defects of the Bjerrum type known in ices. Here we advance an alternative, more generic, interpretation based on a careful calorimetric study of the behaviour of two HQGs and compared it with the endotherm behaviour of annealed HQGW.

Our glasses were both hyperquenched, by melt-spinning from ~2,200 K into ~8-μm fibres at $10^6\,K\,s^{-1}$ (see Methods), a rate comparable to that estimated for the hyperquenching of water[3]. One of our cases was chosen because of its extensive prior characterization[20,21] and the second because it is simple in constitution (Al_2O_3-SiO_2) and, like water, crystallizes almost at T_g. Both are of very high T_g and hence are non-hygroscopic in character and are easily handled or stored.

To examine how glasses that are trapped in high-potential-energy states by hyperquenching recover equilibrium states that lie lower on the potential energy landscape[21], we first characterize a 'standard glass' (a glass obtained by cooling at a rate of $-0.33\,K\,s^{-1}$; see also Fig. 1 caption). Then we compare, with this standard, the standard upscan of the HQG.

Figure 1 shows the thermal behaviour of the hyperquenched samples treated analogously to the HQGW samples, that is, upscanned at the standard rate after being annealed for 90 min at various temperatures well below T_g. The data show that if the annealing temperature (T_a) is sufficiently high, the upscan trace develops an endothermic component whose onset temperature appears to be fixed, but whose peak value depends on the temperature of annealing for a given annealing time (t_a).

In Fig. 2 we select one of these scans and compare it with the scan exhibiting the endotherm attributed in ref. 14 to the glass transition of water. The resemblance is striking, illustrating that it is possible to obtain a trace with the same form (and also the same small ΔC_p) as that attributed to the glass transition of water merely by appropriate annealing of the HQGW. Because the endotherm is determined by the relaxation characteristics of the material in the α-, or primary relaxation region, and is at least qualitatively predictable from the phenomenological models for the α-relaxation[19], we rename it the 'shadow' glass transition with a transition temperature $T_{g,shadow}$, to distinguish it from any β-relaxation that would normally lie at a lower temperature with respect to the standard T_g.

For the crystallization-resistant mineral glass, the T_a can be placed arbitrarily close to the standard T_g, but, in the case of water, attempts to raise T_a much higher than 130 K for $t_a = 90$ min lead to crystallization. This feature explains why the shadow glass transition could be taken for the real transition.

In a recent study[13], microdroplet water was deposited and vitrified at different substrate temperatures. Calorimetric characterization showed that whereas no endotherm appeared for water deposited at 130 K, an endotherm did appear for the sample deposited at 140 K (see Fig. 3b, c). The 45-min deposition process itself establishes a temperature–time history amounting to an average 23-min anneal at the deposit temperature. The usual construction for the onset T_g (Fig. 1) now suggests that glassy water has a T_g higher than inferred before, namely 141 K. We demonstrate, in Fig. 3a, the parallel effect with hyperquenched glassy $35\%Al_2O_3$-$65\%SiO_2$, which is only slightly more stable against crystallization than water.

Figure 3a shows the behaviour of this sample after long isochronal annneals at two different temperatures, 993 and 1,033 K, not far below the standard T_g. The sample annealed at 1,033 K exhibits a shadow peak that has risen to about a quarter the strength of the standard transition at overshoot. The crystallization of this glass can be seen to occur immediately after the overshoot peak of the standard scan. The transition temperature now attributed to the shadow glass transition has increased to 1,120 K, while annealing at 993 K yields a $T_{g,shadow}$ of only 1,063 K. This annealing-induced increase in T_g is 5%, compared to an increase of 4% in the case of water (141 K/136 K). A recent study[18] asserted that the onset temperature of the sub-T_g peak is the same as the annealing temperature. This correlation does not hold for the $T_{g,shadow}$ value we obtain for the annealed HQGs (Fig. 3a), but it does seem to hold for the glassy water deposited and annealed at the higher temperature (Fig. 3b, c).

The behaviour of our two HQGs allows us to closely reproduce the behaviour of annealed HQGW, yet the endotherm of the glasses is only a 'shadow' of the real glass transition, which occurs some 15% higher in temperature. These findings strongly suggest that the water endotherm at 136 K is also only a 'shadow' of the real glass transition, substantiating earlier claims[6] that the real T_g of water cannot be assigned except by some scaling procedure. These results parallel early studies on hyperquenched metallic glasses[22] and have now also been obtained in studies on electrospray-quenched molecular glasses of dibutylphthalate and propylene glycol (L.-M. Wang and C.A.A., unpublished work).

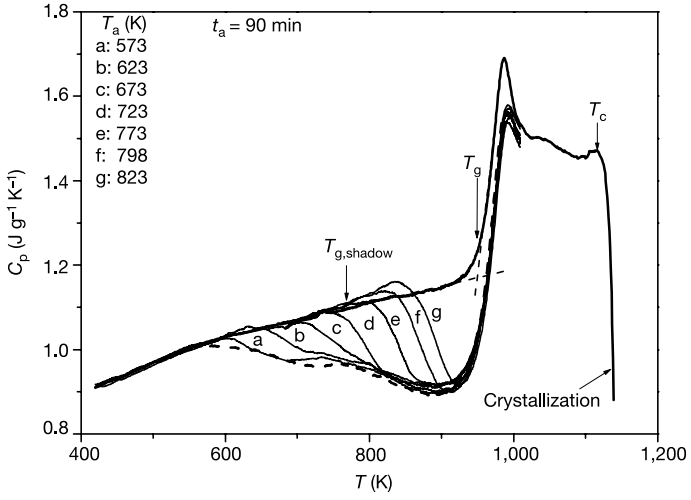

Figure 1 DSC upscans of hyperquenched and annealed HQGs. The thick lines show the comparison of the initial upscan of the hyperquenched glass at the standard rate (thick dashed line), with the upscan of the standard glass (thick solid line). The standard rate of $0.33\,K\,s^{-1}$ was chosen because the 'onset-heating glass temperature' $T_{g,onset}$, defined here from a DSC standard upscan, is then the temperature at which the structural relaxation time is ~100 s (refs 2, 17). The upscan on the standard glass is continued until crystallization occurs at $T_c = 1{,}127$ K. The standard upscan T_g is 944 K from the construction (dashed lines) shown. The quenched-in energy of the HQG is given by the area between the two curves, and is $64\,J\,g^{-1}$. The fictive temperature of the HQG, determined as in refs 6 and 32, is 1,152 K. The thin solid lines (a–g) represent a series of standard upscans of aged samples. For each of lines a to g, a fresh sample of the HQG was annealed for 90 min at the temperature given, in order to observe the enthalpy relaxation of the remaining excess (frozen-in) enthalpy. Note, in particular, the evidence that the samples aged at temperatures above ~723 K reach lower enthalpies than the standard glass for fast-relaxing components of the structure, whereas the slow-relaxing components of the structure are still trapped in states of much higher enthalpy than that of the standard glass. The term $T_{g,shadow}$ is explained in the text.

Reproducibility of the endothermic effect[14] has been one of the supporting arguments resulting in the general acceptance of 136 K as the T_g appropriate to water. We find that the 'sub-T_g peaks' seen with our inorganic glass over the temperature range 710–850 K (Fig. 1) can be reproduced any number of times by repeating the annealing process at the same temperature, provided that the crossover temperature (where endotherm becomes exotherm relative to the standard scan) is not exceeded on heating[20].

The endothermic effect is easily understood[17]. All glasses have a spectrum of relaxation times, as if composed of many microglasses of different T_g values. The structural relaxation of water (though not its dielectric relaxation) has a broad spectrum, as recently determined by optical Kerr-effect studies (R. Torre, personal communication). The shadow T_g is simply the collective T_g of that component of the HQG that has micro-T_g values low enough to be relaxed by the annealing.

Attributing the endothermic effect at 136 K to a sub-T_g peak (annealing pre-peak, or shadow glass transition) explains several perceived inconsistencies in the phase behaviour of glassy water. First, an activation energy (E_a) of 55.5 kJ mol^{-1} has been inferred[3,14,10] for the apparent glass transition relaxation endotherm, yet this value, when considered relative to T_g, is characteristic of a strong liquid[2,10], even though water in this temperature regime is thought to be a fragile liquid[9,11]. Moreover, the E_a is close to the E_a values for relaxation processes in ice, as would be expected if the water is still a glass at 150 K. (Four independent studies of ASW crystallization obtained E_a values ranging from 55–84 kJ mol^{-1}, as reviewed in ref. 23.) Taken together, these considerations suggest that the E_a derived from the 136 K endotherm reflects the diffusion coefficient in the crystallizing phase[24]. If water were a fragile liquid near T_g, this E_a should be >170 kJ mol^{-1} (ref. 9).

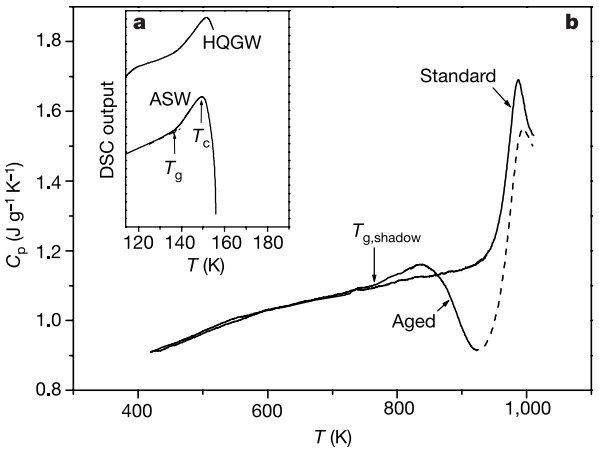

Figure 2 Comparison of DSC upscans of aged, hyperquenched mineral glass with the equivalent water DSC upscans for HQGW and ASW. The thermogram of the hyperquenched mineral glass sample, aged for 90 min at 823 K before upscanning (**b**), is compared with the upscans of HQGW and vapour-deposited ASW samples[14] that had been aged for 90 min at 130 K before upscanning (**a**). The temperature scales are set so that each has 0 K at the same point offscale. The upscans for the water samples have provided the basis for assigning a T_g of 136 K to water. The comparison of **a** with **b** shows that the endotherm in **a** can arise from an annealing effect. The 'real' glass transition in the case of water has been eliminated from observation by crystallization. The dashed line in **b** is the part that we suggest has been cut from the water sample scan by crystallization, commencing at or slightly above the temperature marked T_c. The ratio of $T_{g,onset}$ to T_g of the mineral glass is 0.80. Applying the same ratio to $T_{g,shadow}$ of water we obtain a 'real but hidden' T_g of 169 K. However, this ratio will depend on system fragility, so the estimate of the hidden T_g for water is uncertain, and is better estimated by other means[6,28]. (Data and identification on HQGW and ASW taken from ref. 10, re-plotted from ref. 14.)

As mentioned before, the extremely weak jump in C_p at T_g (see Fig. 2a and refs 3, 14) is 14-fold smaller than expected from extrapolations of ΔC_p data for seven different binary aqueous solutions[2,15]. This apparent contradiction has been explained[10] as being due to water changing from a fragile liquid to a strong liquid as temperature decreases during hyperquenching (or as the binary solutions change composition during dilution at low temperature). But it is not necessary to invoke a fragile-to-strong transition if the weak endotherm is simply an annealing pre-peak, rather than a real glass transition, given the ΔC_p values typically associated with 'shadow' and 'real' glass transitions (see Figs 1–3).

Attributing the long-controversial endothermic effect of glassy water to an annealing effect, not a T_g, also provides a simple explanation for puzzling changes[25] in the T_g of aqueous ethylene glycol (EG) and LiCl solutions, which first decreases and then suddenly increases by about 25 K with increase in EG or LiCl content. This sudden increase in T_g occurs on approach to the composition where the solutions become glassforming on normal cooling, but overshoots the published values owing to the 'normal' annealing effect[17]. (For the dilute compositions in ref. 25, an "optimal annealing temperature" had to be found to distinguish the EG-water 'T_g' from 'sub-T_g' shoulders observed on annealing a variety of glasses"[25]).

One argument for glassy water undergoing a glass transition to supercooled liquid is the observation that that LDA (T_g = 129 K, ref. 26) can be penetrated at 143 K by a blunt probe[8] that penetrates *cis*-decalin (T_g = 137.4 K) at 140 K. The observation is puzzling, given that the dielectric relaxation (loss tangent) data of unannealed ASW, measured up to and through crystallization[27], clearly indicates that no relaxation occurs below 150 K relative to that for well-known glassformers like glycerol and propylene carbonate at their respective T_g values (see figure 4 of ref. 28). But the penetration temperature, 143 K, coincides with the temperature where crystallization is occurring for samples heated at the speed of the penetration measurement (compare with crystallization data in refs 26 and 29)—and mobility clearly increases during crystallization[9].

To conclude, we note that the enthalpy relaxation plots and the

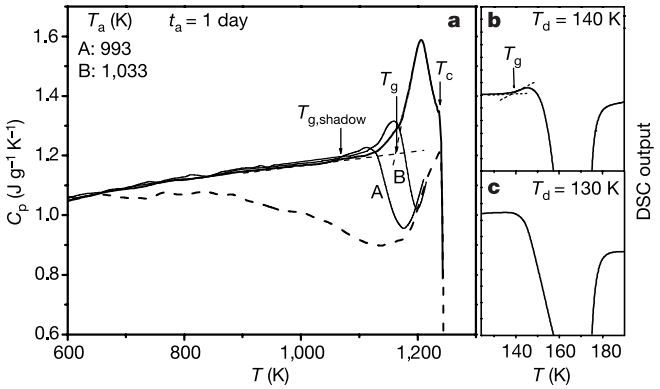

Figure 3 Effect of T_a on shadow glass transitions. **a**, DSC upscans of 35%Al_2O_3-65%SiO_2 standard glass (thick solid line) and HQG (dashed line) compared with two HQGs that had been annealed as in legend, showing shadow transitions (pre-peaks) at temperatures well above annealing temperatures. Shadow transitions increase in both transition strength and onset temperature with increase in T_a values. **b**, **c**, Upscans of vitreous water sample, deposited as 5-μm droplets during 45 min, at temperatures given. The upscan of the deposit at T_d = 130 K (**c**) shows no endotherm before crystallization, while the deposit at T_d = 140 K (**d**) shows an endotherm with onset at 141 K by the usual construction (dashed lines). The shift from the original annealing-induced endotherm at 136 K (labelled T_g of water), is the analogue of the behaviour of the barely stable alumina-silica glass in curve B in **a**. (**b** and **c** are based on data presented in ref. 13.)

shadow glass transition of Fig. 1 give information on, respectively, frozen-in and annealed-out structural fluctuations. Therefore, the type of experiment shown in Fig. 1 may provide much information on water in its pre-vitrification supercooled liquid states. It is, after all, the large mean-square enthalpy fluctuations, responsible for the high heat capacity of supercooled water, that are being frozen-in near the fictive temperature at 200–230 K (ref. 30) during hyperquenching. Such hyperquench-and-anneal studies may also provide important information on water in different structural environments, such as around biomolecules, amphiphiles and the like. Indeed, the enthalpy relaxation and shadow T_g phenomenology may prove much more interesting to water studies than a mere glass transition. □

Methods

Sample preparation

The HQGs of this study were obtained by the cascade melt-spinning process. One sample is a multicomponent mineral (basalt) glass that has been well characterized elsewhere[20]: composition (mol%): 47.5 SiO_2, 9.1 Al_2O_3, 6.6 FeO, 15.9 CaO, 16.9 MgO, 2.0 Na_2O, 0.7 K_2O. The second is from a binary aluminosilicate melt with the composition (mol%): 65 SiO_2, 35 Al_2O_3. Before the spinning, the melts were homogenized at temperatures of about 1,800–1,850 K (for the mineral system) and about 2,173–2,223 K (for the binary system) for half an hour. The fibres were spun using the wheel centrifuge process, which has also been called the cascade or mechanical spinning process[31]. The glass melt is conveyed down a trough and onto the outer rim of a spreader wheel. Although some material is spun off, most of the melt is transferred to either of two larger adjacent wheels that are spinning at 6,000 r.p.m. in the opposite direction. Fibres form when droplets of diameter >65 μm are thrown from the wheels by centripetal force. To remove the remaining glass droplets from the fibre ends, and to ensure uniform fictive temperature and properties, the fibres were separated using a 65-μm sieve. Of the fibre volume, 84 vol.% is of diameter <12.6 μm, 50 vol.% is of $d < 7.7$ μm, and only 16 vol.% have $d < 4.1$ μm. The average hyperquenching rate was estimated to be 2×10^6 K s^{-1}, by calculation from the relation between cooling rate Q and shear viscosity η at the fibre fictive temperature: $\log(1/Q) = \log\eta - 11.35$ (Y.-Z.Y., R. von der Ohe, & S. L. Jensen, unpublished work).

Ageing and calorimetric experiments

Before the DSC measurements, the fibre samples were annealed in an annealing furnace at selected temperatures T_a for $t_a = 90$ min (see Figs 1 and 2), whereas the binary samples were annealed at selected temperatures for 24 h (see Fig. 3). The annealing was performed in air. The apparent C_p of each fibre sample was measured using a Netzsch STA449C DSC. The fibres were placed in a platinum crucible situated on a sample holder of the DSC at room temperature. The samples were held for 5 min at an initial temperature of 333 K, and then heated at a standard rate of 0.333 K s^{-1} to the temperature 1,013 K (for the mineral samples) and 1,236 K (for the binary samples), and then cooled back to 573 K at a rate of 0.333 K min^{-1} to 573 K, thus forming the standard glass. After natural cooling to room temperature, the second upscan was performed using the same procedure as for the first. To determine the C_p of the fibres, both the baseline (blank) and the reference sample (sapphire) were measured. To confirm reproducibility, the measurements for some samples were repeated to check for drift in the baseline.

Received 3 July; accepted 12 December 2003; doi:10.1038/nature02295.

1. Pryde, J. A. & Jones, G. O. Properties of vitreous water. *Nature* **170,** 635–639 (1952).
2. Angell, C. A. Liquid fragility and the glass transition in water and aqueous solutions. *Chem. Rev.* **102,** 2627–2649 (2002).
3. Johari, G. P., Hallbrucker, A. & Mayer, E. The glass transition of hyperquenched glassy water. *Nature* **330,** 552–553 (1987).
4. Johari, G. P. Does water need a new T_g? *J. Chem. Phys.* **116,** 8067–8073 (2002).
5. MacFarlane, D. R. & Angell, C. A. Nonexistent glass transition for amorphous solid water. *J. Phys. Chem.* **88,** 759–762 (1984).
6. Velikov, V., Borick, S. & Angell, C. A. The glass transition of water, based on hyperquenching experiments. *Science* **294,** 2335–2338 (2001).
7. Jenniskens, P., Banham, S. F., Blake, D. F. & McCoustra, M. R. S. Liquid water in the domain of cubic crystalline ice I-c. *J. Chem. Phys.* **107,** 1232–1241 (1997).
8. Johari, G. P. Liquid state of low-density pressure-amorphized ice above its T_g. *J. Phys. Chem. B* **102,** 4711–4714 (1998).
9. Smith, R. S. & Kay, B. D. The existence of supercooled liquid water at 150 K. *Nature* **398,** 788–791 (1999).
10. Ito, K., Moynihan, C. T. & Angell, C. A. Thermodynamic determination of fragility in liquids and a fragile-to-strong liquid transition in water. *Nature* **398,** 492–495 (1999).
11. Kivelson, D. & Tarjus, G. H_2O below 277 K: A novel picture. *J. Phys. Chem. B* **105,** 6620–6627 (2001).
12. Hallbrucker, A. & Mayer, E. Calorimetric study of the vitrified liquid water to cubic ice phase transition. *J. Phys. Chem.* **91,** 503–505 (1987).
13. Kohl, I., Mayer, E. & Hallbrucker, A. The glassy water-cubic ice system: a comparative study by X-ray diffraction and differential scanning calorimetry. *Phys. Chem. Chem. Phys.* **2,** 1579–1586 (2000).
14. Hallbrucker, A., Mayer, E. & Johari, G. P. Glass-liquid transition and the enthalpy of devitrification of annealed vapor-deposited amorphous solid water. A comparison with hyperquenched glassy water. *J. Phys. Chem.* **93,** 4986–4990 (1989).
15. Angell, C. A. & Tucker, J. C. Heat capacity changes in glass-forming aqueous solutions, and the glass transition in vitreous water. *J. Phys. Chem.* **84,** 268–272 (1980).
16. Ghormley, J. A. Enthalpy changes and heat-capacity changes in transformations from high-surface-area amorphous ice to stable hexagonal ice. *J. Chem. Phys.* **48,** 503–511 (1968).
17. Hodge, I. M. Enthalpy recovery in amorphous materials. *J. Non-Cryst. Solids* **169,** 211–266 (1994).
18. Johari, G. P. Water's endotherm, the sub-T_g peak of glasses and T_g of water. *J. Chem. Phys.* **119,** 2935–2937 (2003).
19. Huang, J. & Gupta, P. Enthalpy relaxation in thin glass fibers. *J. Non-Cryst. Solids* **151,** 175–181 (1992).
20. Yue, Y.-Z., Jensen, S. L. & Christiansen, J. de C. Physical aging in a hyperquenched glass. *Appl. Phys. Lett.* **81,** 2983–2985 (2002).
21. Angell, C. A. *et al.* Potential energy, relaxation, vibrational dynamics and the boson peak, of hyperquenched glasses. *J. Phys. Condensed Matter* **15,** S1051–S1068 (2003).
22. Inoue, A., Masumoto, T. & Chen, H. S. Enthalpy relaxation behaviour of metal-metal (Zr-Cu) amorphous alloys upon annealing. *J. Mater. Sci.* **20,** 4057–4068 (1985).
23. Angell, C. A. in *Water Science for Food, Health, Agriculture and Environment* (eds Berk, Z., Leslie, R. B., Lilford, P. J. & Mizrahi, S.) 1–30 (Technomic, Lancaster, 2001).
24. Ngai, K. L., Magill, J. H. & Plazek, D. J. Flow, diffusion and crystallization of supercooled liquids: Revisited. *J. Chem. Phys.* **112,** 1887–1892 (2000).
25. Hofer, K., Hallbrucker, A., Mayer, E. & Johari, G. P. Vitrified dilute aqueous-solutions. 3. Plasticization of waters H-bonded network and the glass-transition temperatures minimum. *J. Phys. Chem.* **93,** 4674–4677 (1989).
26. Johari, G. P., Hallbrucker, A. & Mayer, E. Two calorimetrically distinct states of liquid water below 150 kelvin. *Science* **273,** 90–92 (1996).
27. Johari, G. P., Hallbrucker, A. & Mayer, E. The dielectric behavior of vapor-deposited amorphous solid water and of its crystalline forms. *J. Chem. Phys.* **95,** 6849–6855 (1991).
28. Angell, C. A. Amorphous water. *Annu. Rev. Phys. Chem.* **55,** 559–583 (2004).
29. Handa, Y. P. & Klug, D. D. Heat capacity and glass transition of amorphous ice. *J. Chem. Phys.* **92,** 3323–3325 (1988).
30. Fleissner, G., Hallbrucker, A. & Mayer, E. Increasing contact-ion pairing as a supercooled water anomaly. Estimation of the fictive temperature of hyperquenched glassy water. *J. Phys. Chem. B* **102,** 6239–6247 (1998).
31. Axten, C. W. *et al. Man-made Vitreous Fibers: Nomenclature, Chemical and Physical Properties* (ed. Easters, W.) 17 (TIMA, Inc., Stamford, CT, 1991–1993).
32. Yue, Y.-Z., Christiansen, J. de C. & Jensen, S. L. Determination of the fictive temperature for a hyperquenched glass. *Chem. Phys. Lett.* **357,** 20–24 (2002).

Acknowledgements We are grateful for the support of Rockwool International, Denmark, Department of Production, Aalborg University, Denmark (to Y.-Z.Y.) and for a Solid State Chemistry grant from the National Science Foundation (C.A.A.). We thank S.L. Jensen for help with samples.

Competing interests statement The authors declare that they have no competing financial interests.

Correspondence and requests for materials should be addressed to C.A.A. (caa@asu.edu).

High-latitude influence on the eastern equatorial Pacific climate in the early Pleistocene epoch

Zhonghui Liu & Timothy D. Herbert

Department of Geological Sciences, Brown University, Providence, Rhode Island 02912, USA

Many records of tropical sea surface temperature and marine productivity exhibit cycles of 23 kyr (orbital precession) and 100 kyr during the past 0.5 Myr (refs 1–5), whereas high-latitude sea surface temperature records display much more pronounced obliquity cycles at a period of about 41 kyr (ref. 6). Little is known, however, about tropical climate variability before the mid-Pleistocene transition about 900 kyr ago, which marks the change from a climate dominated by 41-kyr cycles[7] (when ice-age cycles and high-latitude sea surface temperature variations were dictated by changes in the Earth's obliquity[8,9]) to the more recent 100-kyr cycles of ice ages. Here we analyse alkenones from marine sediments in the eastern equatorial Pacific Ocean to reconstruct sea surface temperatures and marine productivity over the past 1.8 Myr. We find that both records are dominated by the 41-kyr